High dynamic range optimal fuzzy color image enhancement using Artificial Ant Colony System

Om Prakash Verma [a,*], Puneet Kumar [b], Madasu Hanmandlu [c], Sidharth Chhabra [d]

[a] Department of Information Technology, Delhi Technological University, Delhi 110085, India
[b] Scientist 'B', Advanced Systems Laboratory, Hyderabad, India
[c] Electrical Engineering Department, IIT Delhi, Delhi, India
[d] Department of Computer Engineering, Delhi Technological University, Delhi 110085, India

ARTICLE INFO

ABSTRACT

This paper presents a novel approach for the enhancement of high dynamic range color images using fuzzy logic and modified Artificial Ant Colony System techniques. Two thresholds, the lower and the upper are defined to provide an estimate of the underexposed, mixed-exposed and overexposed regions in the image. The red, green and blue (RGB) color space is converted into Hue Saturation and Value (HSV) color space so as to preserve the chromatic information. Gaussian MFs suitable for the underexposed and overexposed regions of the image are used for the fuzzification. Parametric sigmoid functions are used for enhancing the luminance components of under and over-exposed regions. Mixed-exposed regions are left untouched throughout the process. An objective function comprising of Shannon entropy function as the information factor and visual appeal indicator is optimized using Artificial Ant Colony System to ascertain the parameters needed for the enhancement of a particular image. Visual appeal is preferred over the consideration of entropy so as to make the image human-eye-friendly. Separate power law operators are used for the saturation adjustment so as to restore the lost information. On comparison, this approach is found to be better than the bacterial foraging (BF)-based approach [1].

1. Introduction

Image enhancement is the process of enhancing the visual information within the image. It improves the image quality for better understanding and perception. The need for the image enhancement is necessitated because of the limited capabilities of the hardware used for capturing the image, the uneven lighting conditions and external disturbances. An efficient image enhancement technique is required in many fields such as computer vision, remote sensing, robot navigation, biomedical image analysis and forensic image analysis.

The popular methods of image enhancement are histogram and transform based techniques, contrast stretching, image smoothing, image sharpening, inverse filtering, Wiener filtering, etc. Some variants of these methods such as space variant luminance maps [2], histogram modification for contrast enhancement [3] and combined contrast enhancement and half-toning [4] have been partially successful, but either of these cannot be generalized for all type of color images. Kokkeong and Oakley [5] deal with enhancing color and contrast in images degraded by atmospheric effects like haze,

fog, mist and cloud that scatter different light wavelengths. Bockstein [6] proposed a color image equalization method for the color image enhancement using Luminance, Hue, and Saturation (LHS) color model [7]. A method for altering the exposure in an image is given by Eschbach and Webster [8], and this works by iteratively comparing the intensity signal with a pair of preset thresholds. The color saturation in natural scene images is altered in [9], by iteratively processing and comparing the average saturation with the preset threshold. An algorithm that separates the color data into chromaticity and brightness, and then processes each of these components with partial differential equations or diffusion flows is presented in [10]. A novel histogram processing algorithm which takes into account the original image pixel distribution in the equalization process is developed in [11]. Hue preserved color image enhancement is presented in [12] and this generalizes the existing gray scale contrast intensification techniques to color images. These methods are not robust as each approach is geared to a particular degraded image. The major three deficiencies present in most of the methods of image enhancement are [13]: (1) color image enhancement applied to the RGB (red, green, blue) color space is inappropriate for the human visual system; (2) the uniform distribution constraint employed is not suitable to the human visual perception; (3) they are not robust, i.e., each technique handles one type of degraded images only. To mitigate these weaknesses a

decision tree-based contrast enhancement algorithm is proposed in [14] to enhance the various color images simultaneously and fusion of images to overcome the deficiencies is employed in [13,15].

There are very limited methods taking into account the human visual system. Huang et al. [16] presented a novel way of tailor-making according to the needs of the human visual system. The perception of the human visual system is a sort of fuzzy in nature in the sense that a certain image is liked to a certain degree. Thus fuzzy sets [17] offer a problem-solving tool between the precision of classical mathematics and the inherent imprecision of the real world using linguistic variables like "good contrast" or "sharp boundaries," "light red," "dark green," etc., called hedges, can be perceived qualitatively by the human reasoning. Hence we are attracted towards the simplicity of a fuzzy system in representing the real world problems. Two important contributions to the field of fuzzy image enhancement merit an elaboration. One is explained in [18] which deals with "IF. . .THEN. . .ELSE" fuzzy rules; and another in [19] which uses rule-based smoothing in which different filter classes are devised on the basis of compatibility with the neighborhood. Limei and Jiansheng [20] proposed a fuzzy method to enhance dark regions and works well with night images whereas in [21] good results for enhancement are produced for fire color images using fuzzy membership functions. But it is not always possible to know the nature of environment in real time which renders this method of limited use. A generalized iterative fuzzy enhancement algorithm for the degraded images with less gray levels and low contrasts is proposed in [22] and it uses the image quality assessment criterion based on the statistical features of the gray-level histogram of images to control the iterative procedure. Hanmandlu et al. [23,24] used fuzzy intensification to enhance images. Sarode et al. [25] used a fuzzy system to enhance HSV image by modeling S and V as Gaussians. S-curve is used in [26] as the transformation function and the parameters of the S-curve are calculated by maximizing the image information through entropy. This approach some times over enhance or under enhance the images as they do not preserve the shape of the original histogram. Yu et al. [27] tried to understand the relationship between intensity and saturation and proposed a new method called SI correction for removing color distortion in the HSV space. Annamaria et al. [28] used scene irradiance map as an image property to enhance the image which are subject to many factors, like the local surface reflectance, occlusion, shadow, etc.

Direct enhancement of the RGB color space is inappropriate for the human visual system since it may produce color artifacts and distort the original color (hue) of the image. Hence, the chromatic and achromatic information should be decoupled, which is the reason for using HSV color space in this paper. Deepak and Joonwhoam [29] proposed a similar approach by working only on the luminance component of HSV color space where the V component is divided into smaller blocks and then uses multiple steps to preserve the details. We propose a method for the automatic enhancement of all types of degraded images. The saturation is varied depending upon the region and luminance, while keeping the hue of the image fixed. The exposure [1] is used for the division of the histogram into two parts underexposed and overexposed. Here we use exposure as the initial value for another variable pivot, which is further used for calculating the lower threshold [LT] and upper threshold [UT] to categorize the image into under, mixed and over-exposed regions. We use GINT as a fuzzification function and sigmoid operator for the enhancement. The parameters of the operators are varied to a particular type of degradation. The minimization of the proposed objective function which is a function of Shannon entropy and visual appeal leads to enhancement of the image by stretching intensity (V) component of pixels about the crossover point. The entropy and visual factor involved in the objective function are optimized using the evolutionary algorithm Artificial Ant Colony

System (AACS). In the case of permanently degraded images, the approach can recover the lost details with saturation enhancement only up to some extent.

The evolutionary algorithm such as Genetic Algorithm (GA) and Bacterial Foraging (BF) has been applied in the field of image enhancement. Shyu and Leou [30] presented an approach based on GA for the color image enhancement, where weighted combination of four types of nonlinear transforms (s-curves) is used as a transformation function. In [1], BF algorithm is used for color image enhancement and the BF is used to optimize the objective function. An another evolutionary algorithm known as Artificial Ant Colony System (described briefly in Appendix A) also called Ant Colony Optimization (ACO) proposed in 1997 by Dorigo and Gambardella [31] is applied in the proposed approach. The main idea is that the self organizing principles, which allow the highly coordinated behavior of real ants, can be exploited to coordinate populations of artificial agents that collaborate to solve computation problems. The first ACO algorithm, called the *ant system*, was proposed by Dorigo et al. [32]. Since then, a number of ACO algorithms have been developed, such as Max–Min ant system [33], ant colony algorithm for solving continuous optimization problem [34], an improved ACO for solving the complex combinatorial optimization problem [35], etc. The direct and derived forms of Ant colony optimization algorithms have been applied to many optimization problems, dynamic problems in real variables, stochastic problems, multi-targets and parallel implementations. Some of them are the application of ACO in classification [5], set problems [36], assignment problems [37], data mining [38], etc. As far as our information is concerned the applications of ACO in the field of image processing is very limited. It is mainly used in the edge detection [39–45] and pose estimation [46]. In the present approach the application of AACS (or ACO) is extended to image enhancement. Here AACS is used to optimize the proposed objective function so as to find the optimized value of the parameters used in the enhancement.

The organization of the paper is as follows. Section 2 introduces image division based upon luminance. Section 3 describes fuzzification, intensification and de-fuzzification of the intensity histogram and enhancement of saturation depending upon the region. Concepts of information factor, visual factor, objective function generation, modified AACS and the complete algorithm of the proposed approach is presented in Section 4. AACS is briefly discussed in Appendix A. Finally the results are discussed in Section 5 and conclusions are drawn in Section 6.

2. Image division based upon intensity distribution

Images of scenes seldom appear natural in comparison to their visual perception; hence histogram of image fails to occupy the whole dynamic range. It is known that when intensity distribution is skewed towards the lower part of the histogram then the region appears darker whereas when it is skewed towards the upper part of the histogram then the image appears brighter. In both the cases, the image is perceived as blurred. The images, in these situations are known to possess a high dynamic range; in that they have regions of underexposed and overexposed. By underexposed or overexposed regions in an image, we mean the region where a group of neighborhood pixels have gray levels very close to either the least or the highest respectively of the available dynamic range. It may be noted that when dealing with color images, only the V component of HSV is utilized for the purpose of delineation of an image histogram into underexposed, mixed-exposed and overexposed regions.

The parameter "*exposure*" [1] which is a measure of intensity exposition in an image is used to categorize the image into different regions. Every image is now considered as a mixed image containing a certain percentage of each type of regions. The parameter

exposure which acts as an initial pivot for the division of an image into the under and over exposed regions is given by,

$$\text{Exposure} = \left(\frac{1}{L}\right)\left(\frac{\left(\sum_{\nu=1}^{L} p(\nu) \times \nu\right)}{\sum_{\nu=1}^{L} p(\nu)}\right) \tag{1}$$

where ν indicates the gray-level of a pixel, $p(\nu)$ denotes the histogram and L represents the number of gray levels in an image. Since a single parameter cannot characterize the under, mixed and over exposed regions of an image, two threshold parameters: upper threshold (UT) and lower threshold (LT) are introduced. All gray levels below UT are assumed to lie in the underexposed region and all gray levels above LT lie in the overexposed region. The remaining pixels lie in the mixed region. Thus we divide the gray levels into 3 parts: $[0:UT-1]$ for the underexposed region $[UT:LT-1]$ for the mixed region and $[LT:L-1]$ for the over exposed region. The two thresholds UT and LT can be expressed in terms of L and three parameters as:

$$UT = L(\gamma - u) \tag{2}$$

$$LT = L(\gamma + l) \tag{3}$$

where γ is the pivot, u lies in the range of 0 to γ and l lies in the range 0 to $(1 - \gamma)$. These parameters are assumed to lie in the range $[0, 1]$. If the values of u and l are close to 0 and γ is close to 0.5, then the image is found to be of pleasing nature. Different operators are defined for the enhancement of the underexposed and overexposed regions. For the mixed type images, processing should be done simultaneously to obtain an image of pleasing nature. Before the start of enhancement, an image is classified into 3 regions and then each region is processed separately. Initially the value of pivot γ is set to *exposure* and its optimum value is found by Artificial Ant Colony System (AACS). In order to simplify the computations, both u and l are set to 0.1.

3. Fuzzification, intensification and enhancement

In this work HSV color model is adopted for the enhancement of an image for its ability to separate the chromatic information from the achromatic. It may be noted that to preserve the original color composition of a color image from becoming an artifact, its hue (H) component should not be altered. As the image information is vague, it is very difficult to determine whether a pixel should be made darker or brighter from its original intensity level for the sake of enhancement; it is only possible under the realm of fuzzy logic that deals with uncertainty. Before we begin enhancing the image, some measures of quality should be set to ascertain the goodness of an image, e.g. whether the image is pleasing or has better appearance indicated by high contrast or low fuzziness. A human observer cannot judge the level of contrast quantitatively as the visual assessment is only subjective. So we resort to fuzzy approaches that handle vagueness and uncertainty of images efficiently by associating a degree of belonging to a particular property; be it an intensity or contrast.

An image of size $R \times C$ in RGB converted into HSV having intensity levels ν_{rc} in the range $[0, L-1]$, can be considered as a collection of fuzzy singletons in the fuzzy domain. Accordingly, the fuzzy representation of an image is

$$I = \cup\{\mu(\nu_{rc})\} = \cup\left\{\frac{\mu_{rc}}{\nu_{rc}}\right\} \tag{4}$$
$$r = 1, 2, 3 \ldots R; c = 1, 2, 3 \ldots C$$

where R and C are the number of rows and columns respectively of an image matrix, $\mu(\nu_{rc})$ or μ_{rc}/ν_{rc} denotes the membership function (MF) μ_{rc} of some property, say, the color intensity level at $(r,$

$c)$th pixel, ν_{rc}. However in the proposed approach, the MFs are associated with only the luminance component $\nu \varepsilon \{V\}$ as we preserve other color components. Moreover to achieve the speed of computation, the histogram of V is utilized for the fuzzification of only the gray levels present in an image thus eliminating the need of converting each pixel's luminance component.

As the image can be split up into three regions based on the values of UT and LT, the fuzzification can be performed on each region separately. For the purpose of fuzzification the distributions in both the regions (underexposed and overexposed) are assumed to be Gaussian. A modified Gaussian Membership Function [1] is used for the fuzzification of the underexposed region as follows:

$$\mu_u(\nu) = e^{-[(\nu_{\max} - (\nu_{avg} - \nu))/(\sqrt{2}f_h)]^2} \tag{5}$$

where ν indicates a gray level in the underexposed region in the range $[0, UT-1]$, ν_{avg} is the average gray level and $\nu_{\max}$ is the maximum gray level in the image. f_h is called the fuzzifier and its initial value is found from.

$$f_h^2 = \left(\frac{1}{2}\right)\left(\frac{\sum_{\nu=0}^{L-1}((\nu_{\max} - \nu)^4)p(\nu)}{\sum_{\nu=0}^{L-1}((\nu_{\max} - \nu)^2)p(\nu))}\right) \tag{6}$$

The mirror function of the above Gaussian MF is used to fuzzify the overexposed region of the image for $\nu \geq LT$ as follows:

$$\mu_o(\nu) = e^{-[(\nu_{\max} - (\nu_{avg} - (L-\nu)))/(\sqrt{2}f_h)]^2} \tag{7}$$

The choice of the mirror function is made because of the need to eliminate the stacked upper intensity levels.

It may be noted that the above MFs are selected to be mutually exclusive and pertain to the respective regions. The fuzzification function in (5) operates below the upper threshold and that in (7) operates above the lower threshold, whereas the region between the upper and lower threshold is left untouched.

Just as different fuzzification functions, we use different operators of sigmoid function type for enhancing the underexposed and overexposed regions. A parametric sigmoid function [47] (or simply sigmoid operator) for enhancing the MF values in the underexposed region is given by:

$$\mu_u'(\nu) = \left\{\frac{1}{1 + e^{-t(\mu_u(\nu) - \mu_{cu})}}\right\} \tag{8}$$

And that for enhancing the overexposed region is

$$\mu_o'(\nu) = \left\{\frac{1}{1 + e^{-g(\mu_o(\nu) - \mu_{co})}}\right\} \tag{9}$$

where t and g are intensification parameters (or intensifiers) and μ_{cu} and μ_{co} are the crossover points for under and over exposed regions respectively. The above operators modify the MFs and the modified MFs are de-fuzzified by using the respective inverse MFs. Next we need to combine the three regions to make up the enhanced image. For this, firstly the de-fuzzified gray levels in the underexposed region are translated and scaled to lie in between $[0, UT-1]$, and those in the overexposed region are translated and scaled to $[LT, L-1]$, and the region between $[UT, LT-1]$ is taken from the original histogram and these are combined into a single region.

Enhancement of saturation is necessitated in restoring the lost details of an image. As the value of saturation is reduced, the image regains its pleasing nature in the underexposed region whereas increasing the saturation helps the overexposed region. Blindly enhancing saturation may lead to loss of useful information. A way out to this problem is to increase the saturation depending upon whether a pixel is made darker or brighter.

When an image is overexposed then it underestimates the saturation component and reverse is the case when overexposed. Therefore pixels lying in the underexposed region should have

their saturation reduced and those lying in the overexposed region should have their saturation increased. Hence we introduce two power law operators given by

$$I_o'(S) = [I_o(S)]^{S_O} \quad \forall \text{ pixels in the overexposed region} \tag{10}$$

$$I_u'(S) = [I_u(S)]^{S_u} \quad \forall \text{ pixels in the underexposed region} \tag{11}$$

where S_o and S_u are the saturation intensifier and de-intensifier chosen experimentally. I_u and I_u' denote the original and the modified saturation components of HSV color model for the underexposed region; likewise I_u and I_o' are the corresponding saturation components for the overexposed region.

4. Measurement of fuzziness and optimization

4.1. Fuzzy contrast measure

Measures of image appearance such as contrast and visual factors are required to be coined for judging the image quality. Perception of image quality by the human visual system is subjective. Hence it is very difficult to find an appropriate quality measure matching the perceptual assessment of the human visual system. A fuzzy approach comes to rescue here in finding a suitable measure of image quality. The performance of this approach can be measured objectively by the quantitative analysis of an image and subjectively by the visual analysis.

The entropy and visual factors can be used as a qualitative measure of image quality. The fuzzy contrast of an image is found by measuring the deviation of the membership values of luminance components of pixels of an image from the crossover point. Separate fuzzy contrasts are defined for the underexposed and the overexposed regions and none for the mixed region.

The fuzzy contrast for the underexposed region of the image is given by:

$$C_u = \left(\frac{1}{UT}\right)\left(\sum_{\nu=0}^{UT-1}(\mu_u'(\nu) - \mu_{cu})^2\right) \tag{12}$$

The average fuzzy contrast for the underexposed region of the image is computed as:

$$\bar{C}_u = \left(\frac{1}{UT}\right)\left(\sum_{\nu=0}^{UT-1}(\mu_u'(\nu) - \mu_{cu})\right) \tag{13}$$

The fuzzy contrast for the overexposed region of the image is

$$C_o = \left(\frac{1}{L-LT}\right)\left(\sum_{\nu=LT}^{L-1}(\mu_o'(\nu) - \mu_{co})^2\right) \tag{14}$$

The average fuzzy contrast for the overexposed region of the image

$$\bar{C}_o = \left(\frac{1}{L-LT}\right)\left(\sum_{\nu=LT}^{L-1}(\mu_o'(\nu) - \mu_{co})\right) \tag{15}$$

The corresponding initial fuzzy contrasts of two regions with respect to the crossover point before enhancing the membership values are:

$$C_{ui} = \left(\frac{1}{UT}\right)\left(\sum_{\nu=0}^{UT-1}(\mu_u(\nu) - \mu_{cu})^2\right) \tag{16}$$

$$\bar{C}_{ui} = \left(\frac{1}{UT}\right)\left(\sum_{\nu=0}^{UT-1}(\mu_u(\nu) - \mu_{cu})\right) \tag{17}$$

$$C_{oi} = \left(\frac{1}{L-LT}\right)\left(\sum_{\nu=LT}^{L-1}(\mu_o(\nu) - \mu_{co})^2\right) \tag{18}$$

$$\bar{C}_{oi} = \left(\frac{1}{L-LT}\right)\left(\sum_{\nu=LT}^{L-1}(\mu_o(\nu) - \mu_{co})\right) \tag{19}$$

As per our definition, the fuzzy contrast measures the spread of the membership gradient with respect to the crossover point and the average fuzzy contrast denotes the overall intensity of the image. Their ratio called the quality factor should give some measure of the image quality as a characteristic of an image and is also the basis for visual factor to be defined subsequently.

Definition. The quality factor of an image is calculated as the absolute ratio of the average fuzzy contrast to the fuzzy contrast. The quality factors for both the underexposed and the overexposed region are defined in one equation as:

$$Q_{u/o} = \left|\frac{\bar{C}_{u/o}}{C_{u/o}}\right| \tag{20}$$

The above definition represents the uncertainty present in an image whereas the memberships function depicts the uncertainty in the intensity values. Following (20), the initial quality factors for both the underexposed and the overexposed regions of the image can be written as:

$$Q_{ui/oi} = \left|\frac{\bar{C}_{ui/oi}}{C_{ui/oi}}\right| \tag{21}$$

4.2. Visual factors

For judging the image quality, we now define the normalized contrast factor, called the visual factor. It measures the improvement in visual appearance due to enhancement. Visual factors are separately calculated for the underexposed and the overexposed regions and are combined with weights proportional to the thresholds of the regions. The visual factor for the underexposed region of the image is defined as:

$$V_u = \frac{Q_u}{Q_{ui}} \tag{22}$$

The visual factor for the overexposed region of the image is

$$V_o = \frac{Q_{oi}}{Q_o} \tag{23}$$

These factors are used to ascertain the visual assessment of both the regions. They measure the relative changes in the quality of the regions because of enhancement with respect to the original contrast. Note that from (22) and (23) the visual factor for the overexposed region is inversely defined to that of the underexposed region because its original quality factor is higher than that after enhancement. The weighted sum of the underexposed and overexposed visual factors is taken as the overall visual factor:

$$V_f = \left(\frac{UT}{L}\right)V_u + \left(1 - \frac{LT}{L}\right)V_o \tag{24}$$

It acts as a control over the enhancement of the image. Increasing it beyond a limit causes the loss of information thus degrading the pleasing nature of the image. Empirically, the visual factor is found to be dependent on the initial exposure as follows:

$$V_{sf} \rightarrow 1.5 - \left(\frac{0.9}{255}\right)\gamma_i \tag{25}$$

where γ_i is the initial value of the pivot, i.e. *exposure*, and V_{sf} lies in the range of 0.6–1.5.

4.3. Information factor

Shannon entropy function is a measure of uncertainty involved in the modified membership functions of both under and over exposed regions of an image, expressed as:

$$E = \left(-\frac{1}{L \ln 2}\right)\left[\left(\sum_{v=0}^{UT-1}\{\mu_u'(v)\ln(\mu_u'(v)) + (1-\mu_u'(v))\ln(1-\mu_u'(v))\}\right)\right.$$
$$\left. + \left(\sum_{v=LT}^{L-1}\{\mu_o'(v)\ln(\mu_o'(v)) + (1-\mu_o'(v))\ln(1-\mu_o'(v))\}\right)\right] \quad (26)$$

The entropy function contains four unknown parameters (t, g, f_h, γ) which need to be estimated. This requires framing of a suitable objective function consisting of the entropy and visual factors both of which are important for judging the image quality.

4.4. Objective function for minimization

As noted above that the Shannon entropy function provides a measure of the uncertainty in the enhanced image whereas the difference in the visual factors is associated with the change in the image perception as a result of enhancement. Therefore their combination should serve as an objective function. For this we formulate a constrained optimization problem stated as:

Minimize the entropy function
Subject to constraint $V_f \approx V_{sf}$

where V_{sf} is the desired (or soothing) visual factor whose attainment is a measure of pleasing nature of images. The above optimization leads to the setting up of an objective function J that stresses on the visual appeal of the form:

$$J = E + \lambda e^{|V_f - V_{sf}|} \quad (27)$$

where λ is the Lagrangian multiplier. The optimization of the objective function is done by varying the parameters $1 < t < 10$, $1 < g < 10$ and $0 < \gamma < 255$. The need for the Lagrangian multiplier is eliminated as different values of λ have no significant bearing on the parameters. For the sake of simplicity we take $\lambda = 1$ to give equal weights for the two terms on the right hand side of Eq. (27). We will now present an evolutionary learning technique, viz., Artificial Ant Colony System (AACS) [49,31] that finds the unknown parameters by optimizing the objective function given in Eq. (27). A brief description of the AACS is relegated to Appendix A. However the aspects of implementation of the modified AACS are detailed now.

4.5. The modified AACS

Artificial Ant Colony System is modified to solve a continuous optimization problem expeditiously. The modifications made are: (1) instead of local minimum value, global minimum value is used for faster results, (2) an ant dies as soon as it fails to find food for itself, and (3) pheromone is updated after some K cycles. These steps reduce the complexity and hence speed up the algorithm (see Appendix A).

The selection of the initial parameters of the algorithm such as the number of ants, the precision needed in the determination of
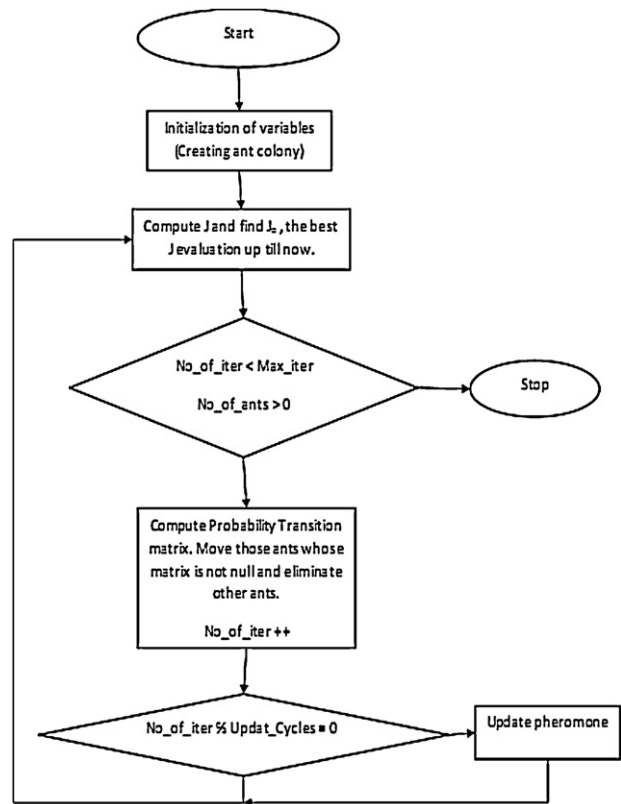

Fig. 1. Flowchart of AACS optimization problem.

parameters (n_p) and the updation time (in number of cycles) plays a key role in arriving at the optimum values in lesser time. These parameters are not standard for all applications but rather depend upon the application. The flowchart of the modified AACS is shown in Fig. 1.

4.6. Initialization of parameters

This includes two sets of parameters: parameters (n_p) of the objective function, i.e. t, g, f_h and γ and the parameters of AACS which make J a time varying function during the learning through optimization. The initialization of parameters of AACS is given in Table 1.

It is possible to achieve a considerable saving of time by reducing the number of ants without any loss of the image quality. The two control parameters α and β used in AACS have different influence on the algorithm. If $\alpha = 0$, this corresponds to a classical stochastic greedy algorithm with multiple starting points since ants are initially randomly distributed on the nodes [48]. On the contrary if $\beta = 0$, only pheromone amplification takes place; this method tends towards stagnation, in which all ants make the same tour, which is sub-optimal [49]. An appropriate trade-off has to be struck between the heuristic value and trail intensity. Therefore we choose $\alpha = 1$ and $\beta = 1$ to lie between two extremes. The attenuation of trail coefficient is fixed at $\rho = 0.9$ so that the ant colony keeps the past history thus preventing the mistakes from being committed.

Table 1
Initialization of parameters of AACS.

N_a (number of ants)	Max_iter (maximum cycles)	Updat_cycles (for pheromone updation)	Precision for determination of n_p	N_runs (number of runs)
20	500	5	0.1	1

4.7. Algorithm 1(Image I)

Step 1. Convert I from RGB to HSV.

Step 2. Compute the histogram $p(v)$ where $v \in \{V\}$.

Step 3. Compute the initial value of f_h using Eq. (6).

Step 4. Compute the values of exposure, pivot (γ_i), upper threshold (*UT*) and lower threshold (*LT*) using Eqs. (1), (2) and (3).

Step 5. Classify the intensity histogram into 3 regions: Under, Mixed and Over exposed.

Step 6. Fuzzify *V* to get $\mu_u(v)$ and $\mu_o(v)$ using Eqs. (5) and (7) respectively.

Step 7. Set both μ_{cu} and μ_{co} to 0.5 and *t* and *g* to random values and then calculate C_{ui}, $\bar{C}_{ui}$, C_{oi}, $\bar{C}_{oi}$, Q_{ui} and Q_{oi} as given in Section 4.1.

Step 8. Enhance the fuzzy membership values using the corresponding sigmoid functions for the underexposed and overexposed regions using Eqs. (8) and (9) respectively without altering the mixed region.

Step 9. Now calculate C_u, $\bar{C}_u$, C_o, $\bar{C}_o$, Q_u and Q_o from the modified membership values as given in Section 4.1.

Step 10. Compute the entropy E and visual factor V_f using Eqs. (26) and (24) by setting the soothing visual factor as:

$$V_{sf} \rightarrow 1.5 - \left(\cdot \frac{9}{255} \right) \gamma_i.$$

Step 11. Compute the objective function using Eq. (27) and optimize it using the modified AACS and find the optimized values of the parameters.

Step 12. Use the optimized values of the parameters as obtained in Step 11 to enhance the fuzzy membership values using the sigmoid operators of the under and over exposed regions.

Step 13. Defuzzify the enhanced fuzzy membership values using their inverse functions and then scale them in their corresponding under and over exposed regions to obtain the gray levels and then combine them to get

$$v = \begin{cases} \mu_u'^{-1}(v) & \forall v < UT \\ v & \forall LT > v \geq UT \\ \mu_o'^{-1}(v) & \forall L > v \geq UT \end{cases}$$

Step 14. Set s_u to 3/4 and s_o to 4/3 for enhancing the saturation in two regions taking account of the exposition.

Step 15. Now convert back the HSV color space image into corresponding RGB color space.

5. Results and discussion

The proposed approach has been implemented on Intel Core 2 CPU at 1.66 GHz using MATLAB version 7.8.0.347. Around more than 50 images of three types (underexposed, mixed and overexposed) taken from real scenarios are considered as test images. A direct application of the operators on the image leads to the binarization of the image. To avoid this situation, the amount of enhancement is controlled by learning the parameters (t, g, f_h and γ) using the optimization of the objective function. The sigmoid operators enhance as well as reduce the luminance depending upon the region they operate on; because of this, discontinuities are observed at the thresholds upperthreshold (*UT*) and lowerthreshold (*LT*). These discontinuities cause unexpected blurring of the image. To get rid of this, the values of operators are increased/reduced until discontinuities disappear. Histogram curves of image "Window" appear in Fig. 2 showing the modified and original intensity distributions. Note that the proposed approach preserves the histogram modes of the image. These curves are different for different images, depending on the nature of the images and the type of operators used.

For the subjective evaluation of the appearance, a few of the test images are shown in Figs. 6(a)–(d), 7(a)–(d) and 8(a)–(d) and those of "Rose," "Camera," and "Village" are shown in Figs. 3–5. Figs. 3–5 present a comparison between the proposed approach and the existing BF-based approach [1]. BF-based approach enhances the mixed-type images but the proposed approach carries out the enhancement to the level of more pleasing. Figs. 9–12, namely, "Sun-trees", "Road", "Rose" and "Village", present a comparison between the enhanced images with and without saturation operator. As mentioned before the underexposed images usually have higher saturation values than the desired they need to be toned down as in "Sun-trees" and "Road". Coming to the overexposed images, "Rose" and "Village" being permanently degraded they contain only very high gray levels. The sole enhancement in this case is not enough to produce a good image. The details in these areas can be recovered to some extent through the restoration of saturation using the saturation operator. The proposed approach gives the results with and without the application of saturation operator on the degraded regions.

Table 2 gives the optimized parameters (t, g, f_h and γ), visual factors, entropy and time taken for the minimization of the objective
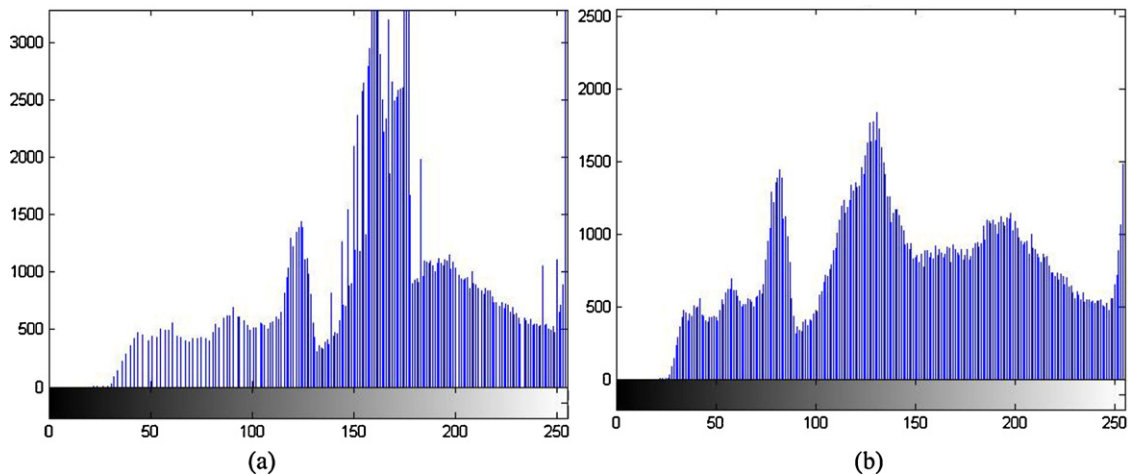

Fig. 2. (a) Original intensity histogram, (b) intensity histogram of the enhanced image of "Window" with the proposed approach.

Fig. 3. (a) Original image, (b) enhanced image of "Rose" with the proposed approach and (c) enhanced Image using BF-based approach.

Fig. 4. (a) Original image, (b) enhanced image of "Camera" with the proposed approach and (c) enhanced Image using BF-based approach.

Fig. 5. (a) Original image, (b) enhanced image of "Village" with the proposed approach and (c) enhanced image using BF-based approach.

function J. Note that the visual factors V_u and V_o indicate the amounts of enhancement achieved on the underexposed and the overexposed regions respectively. A value of 1 means that the initial quality factor and the quality factor after enhancement are the same therefore represents no enhancement. In Table 2, a value of $V_o = 0.9849$ (∼1) for the image "Sun-trees", Fig. 9(a), indicates that there exists very less overexposed region so that the quality factor

after enhancement is almost the same as that of before enhancement. Likewise in case of Fig. 6(d), "baby", $V_o = 0$ indicates that the overall intensity of the "baby" image in the overexposed region is zero. Therefore the sigmoid operator as given in Eq. (9) is not applied on this image as it has no overexposed region. The visual factors seem to serve as good indicators of the effect of enhancement on the appearance of an image, which is difficult to find
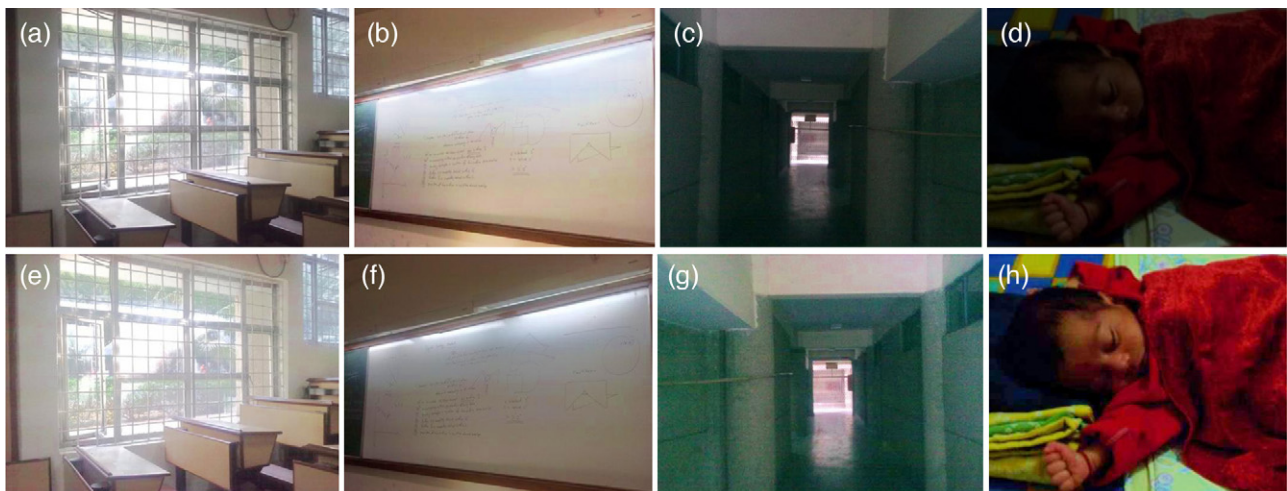

Fig. 6. (a)–(d) The original images and (e)–(h) the enhanced images of them using proposed approach.

Fig. 7. (a)–(d) The original images and (e)–(h) the enhanced images of them using proposed approach.

Fig. 8. (a)–(d) The original images and (e)–(h) the enhanced images of them using proposed approach.

visually at times. The objective assessment of the visual appearance is compared in Table 3 where the visual factors are closer to the soothing visual factor than those obtained using BF-based approach [1]. The execution time gets faster in this approach as compares to BF-based approach. The effect of different population size of ants is also shown in Table 4. We can see that as the

number of ant increases the time taken also increases remarkably but the value of the optimization function decreases. This means that the function is better optimized and will give better results. After some time, even if we increase the ant population size the value of objective function remains the same but the time taken increases. Therefore we can have the same quality of result even

Fig. 9. (a) Original image, (b) enhanced image of "Sun-trees" without saturation enhancement and (c) enhanced image of "Sun-trees" with saturation enhancement.

Fig. 10. (a) Original image, (b) enhanced image of "Road" without saturation enhancement and (c) enhanced image of "Road" with saturation enhancement.
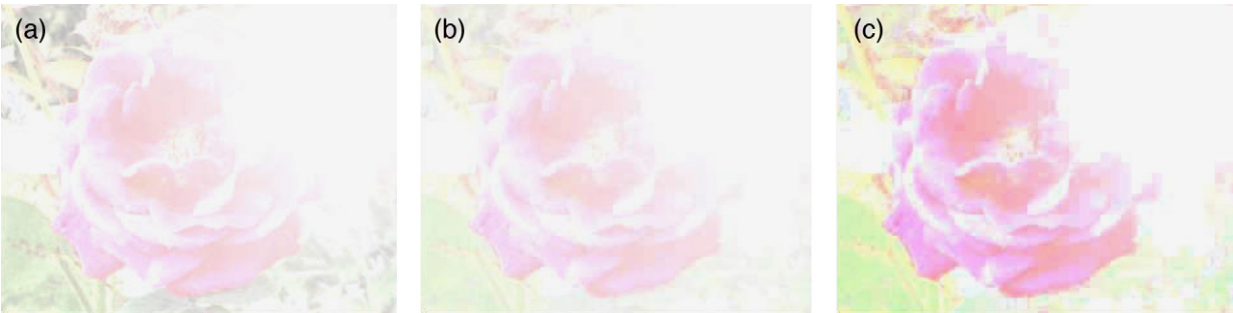

Fig. 11. (a) Original image, (b) enhanced image of "Rose" without saturation enhancement and (c) enhanced image of "Rose" with saturation enhancement.

Fig. 12. (a) Original image, (b) enhanced image of "Village" without saturation enhancement and (c) enhanced image of "Village" with saturation enhancement.

Table 2
Optimization of $J = E + \lambda e^{|Vf - Vsf|}$ with $V_{sf} \rightarrow 1.5 - (\cdot(9/255))\gamma$.

Test image	Size	t	g	f_h	γ	E	V_u	V_o	V_{sf}	V_f	Time elapsed (s)
Rose Fig. 3(a)	330 × 264	9	10	153	150	0.2693	0.9002	0.4025	0.6952	0.6941	50.42
Camera Fig. 4(a)	600 × 450	10	1	120	203	0.4385	1.4087	0.8786	1.3004	1.2989	100.66
Village Fig. 5(a)	600 × 401	30	5	92	64	0.5465	0.2092	0.9536	0.6714	0.7675	121.37
Window Fig. 6(a)	384 × 512	22	10	123	178	0.4094	0.8357	1.2186	0.9538	0.9524	45.23
Board Fig. 6(b)	512 × 384	6	9	153	140	0.4658	1.3165	1.0517	1.0941	1.1024	67.5
Corridor Fig. 6(c)	512 × 384	6	3	150	247	0.5011	1.3191	0.9572	1.3049	1.3064	110.16
Baby Fig. 6(d)	386 × 386	26	10	62.3248	128	0.1481	2.8617	0	0.691	0.0112	47.34
Puneet Fig. 7(a)	942 × 768	100	9	123.7217	128	0.3590	0.2766	1.0924	1.03	1.0893	130.4
Sun-trees Fig. 9(a)	461 × 615	7	2	86	239	0.5226	1.2545	0.9849	1.2471	1.2366	88.99
Road Fig. 10(a)	308 × 410	12	8	104	136	0.6076	1.2936	1.1580	1.2105	1.2301	48.65

Table 3
Comparison of visual factors of proposed approach with BF-based approach.

Test image	V_{sf}	V_f of the BF-based [17] approach	Time taken by the BF based approach	V_f of the proposed approach	Time taken by the proposed approach
Rose Fig. 3(a)	0.6952	1.6009	190.6	0.6941	50.42
Camera Fig. 4(a)	1.3004	1.4230	253.8	1.2989	100.66
Village Fig. 5(a)	0.6714	1.5114	148.6	0.7675	121.37

Table 4
Effect of variation of number of ants for Fig. 7(d).

Number of ants	Time	V_f	V_{sf}	E	J
5	10	1.091	0.9212	0.4	1.585068
10	18	1.09	0.9212	0.38	1.563883
15	28	1.08	0.9212	0.37	1.542104
20	39	1.092	0.9212	0.3	1.486253
25	46	1.094	0.9212	0.309	1.497628
30	48	1.094	0.9212	0.309	1.497628

with the less number of ants. Hence the number of ants should be selected based on the time permitted and the quality required.

6. Conclusions

An image may be categorized into underexposed, mixed-exposed and overexposed regions based on the exposition parameter before carrying out the region-wise enhancement using a fuzzy approach. In this the luminance component of the color intensity property of an image is fuzzified and the hue component was preserved. Gaussian MFs (GINT) suitable for the underexposed and overexposed regions of the image are devised for the fuzzification. Enhancement of the under and overexposed regions is undertaken by the two generalized intensification operators, GINT of sigmoid type, which depend on the crossover point and the intensification parameter. The optimum values of these parameters are obtained by the optimization of the proposed objective function using the modified AACS that involves an iterative learning. The proposed approach produces an enhanced image which is visually more pleasing. The results have been compared with the recent BF-based approach and are found to be better. The presented approach is faster than the BF-based approach. For the case of permanently degraded images, the approach can recover the lost details with the enhancement of saturation only to some extent. For the complete recovery, replacement of information drawn from a similar texture patch is suggested in [20].

Several contributions made as part of this work include: (1) demarcation of an image into underexposed, mixed and overexposed regions; (2) presentation of efficient MF's and operators for the enhancement and objective measures for the assessment of the image quality achieved; (3) presented and verified an effective objective function to get visually appealing images and (4) modification of AACS for improving its computational efficiency.

Appendix A.

The Artificial Ant Colony System also called Ant colony optimization was proposed in 1997 by Dorigo and Gambardella [31] inspired from the observation of the behavior of real ants, for solving the optimization problems with continuous parameters. Ants are social insects residing in colonies. Behavior of ants is determined by the survival of the whole colony, individual ants are less important. Ants can cooperate effectively to finish tasks. For instance even blind ants can find shortest route paths from their colony to feeding sources and back. It was observed that a moving ant deposits pheromone on the ground, hence marking the path it follows. Next ants moving towards the feeding area can identify the pheromone left by the previous ants, decide with high probability to follow it, and reinforce the selected trail with its own pheromone. This form of indirect communication mediated by laying pheromone is known as stigmergy. It is considered that ants make use of pheromone in order to find a shortest path between two points connected with two branches: the shorter and the longer. Ants start from decision points, since there is no initial pheromone. They are free to choose their initial path hence decide randomly. Apparently the ants reaching the source of food faster are able to deposit more

amount of pheromone. This important feature of real ant's behavior is called positive feedback mechanism.

In an Artificial Ant Colony System developed by imitating the real ant's behavior, ant chooses its next step depending upon the transition probability matrix which is a function of the amount of pheromone on the path and the heuristic factor, e.g. the distance between the points. When all the ants have gone through K iterations, then we update pheromone on the path an ant has travelled depending upon how much it has been able to reach towards the objective. The amount of pheromone attenuates gradually along with time. We now assume that there are M ants constituting an ant colony. Initially at $t = 0$, let the value of the pheromone present on each edge be $\tau_{ij}(0)$. In K iterations, each ant moves through a distance making a route. The pheromone deposited on every route is computed from:

$$\tau_{ij}(k+1) = \rho \tau_{ij}(k) + \Delta \tau_{ij}(k+1) \tag{A.1}$$

$$\tau_{ij}(k+1) = \begin{cases} \dfrac{Q}{Lm} & \text{if ant uses edge } ij \text{ in its route} \\ 0 \end{cases} \tag{A.2}$$

where $0 < \rho < 1$ is a coefficient that represent the attenuation of trail. Q is a positive constant. L_m is the length of the route which an ant has traversed in its tour. Now every ant computes its transition probability matrix, $P_{ij}(t)$ and takes a step according to it given by:

$$P_{ij}(t) = \left\{ \frac{([\tau_{ij}(t)]^{\alpha})([\eta_{ij}]^{\beta})}{\sum_{ij \, \varepsilon \, \text{allowed}_{ij}}(([\tau_{ij}(t)]^{\alpha})([\eta_{ij}]^{\beta}))} \right\} \tag{A.3}$$

When η_{ij} is the heuristic factor, allowed$_{ij}$ is the set of points available, α and β are two application dependent parameters that control the relative importance of the two main factors $\tau_{ij}(t)_j$ and η_i.

To optimize an objective function, firstly the size of the ant colony is determined depending upon the constrained field of the problem and precision needed in the computation of parameters. The size of the ant colony is defined as: $M^{PQRS \cdots}$ where P, Q, R, S, etc. are the cardinalities of the sets of values each parameter in n_p can take and M is the number of ants (e.g. if $n_p = 2$, bestows us the two dimensional space as the size of the ant's field restricted by the set of values that those parameters can take).

Secondly the initial pheromone on each edge is set to unity, i.e. $\tau_{ij}(0) = 1$. A heuristic factor for the algorithm is derived from the objective function by:

$$\eta_{ij} = \Delta J_{ij} \tag{A.4}$$

$$\Delta J_{ij} = \begin{cases} J_o - J_{ij}, & J_o \leq J_{ij} \\ 0, & J_{ij} > J_o \end{cases} \tag{A.5}$$

J_o is the best evaluation till now. J_{ij} is the evaluation value at the position ij. Note that ij is a point in the multidimensional space. Transition probability matrix is obtained for every ant and those ants whose matrix remains null are not moved. When all ants have stopped moving it means that we have reached the minima.

A.1. Algorithm_2 (objective function J, parameters n_p)

Step 1. Create an initial distribution of ants in the multidimensional space both deterministically and randomly. Choose those parameters in (n_p) randomly if they are not specified during initialization.

Step 2. For every ant, calculate the value of J and subsequently find J_o and also compute the transition probability matrix P.

Step 3. Eliminate the ants with the transition probability matrix null, i.e. all the elements are 0. Move other ants by a step.

Step 4. Update the pheromone present at each edge according to Eq. (A.5) after the number of "Updat_cycles".

Step 5. Move to the next step else go back to Step 2 if the number of iterations > Max_iter or if no ant has survived

Step 6. Return the best result.

References

[1] M. Hanmandlu, O.P. Verma, N.K. Kumar, M. Kulkarni, A novel optimal fuzzy system for color image enhancement using bacterial foraging, IEEE Trans. Inst. Meas. 58 (8) (2009) 2867–2879.

[2] S. Lee, H. Kwon, H. Han, G. Lee, B. Kang, A space-variant luminance map based color image enhancement, IEEE Trans. Consum. Electron. 56 (November (4)) (2010).

[3] T. Arich, S. Dikbas, A histogram modification framework and its application for image contrast enhancement, IEEE Trans. Image Process. 18 (September (9)) (2009) 1921–1933.

[4] W. Kao, J. Ye, M. Chu, C. Su, Image quality improvement for electrophoretic displays by combining contrast enhancement and halftoning techniques, IEEE Trans. Consum. Electron. 55 (February (1)) (2009) 15–19.

[5] K.K. Tan, J.P. Oakley, Physics-based approach to color image enhancement in poor visibility conditions, J. Opt. Soc. Am. A 18 (2001) 2460–2467.

[6] I.M. Bockstein, Color equalization method and its application to color image processing, J. Opt. Soc. Am. A 3 (5) (1986) 735–737.

[7] R.C. Gonzalez, R.E. Woods, Digital Image Processing, Addison-Wesley, Reading, MA, 1992.

[8] R. Eschbach, N.Y. Webster, Image-dependent exposure enhancement, U.S. Patent [19], Patent Number 5,414,538 (May, 1995).

[9] R. Eschbach, B.W. Kolpatzik, Image-dependent color saturation correction in a natural scene pictorial image, U.S. Patent [19], Patent Number 5,450,217 (September, 1995).

[10] B. Tang, G. Sapiro, V. Caselles, Color image enhancement via chromaticity diffusion, IEEE Trans. Image Process. 10 (May (5)) (2001) 701–707.

[11] J. Duan, G. Qiu, Novel histogram processing for colour image enhancement, in: Proc. Third International Conference on Image and Graphics, 2004, pp. 55–58.

[12] S.K. Naik, C.A. Murthy, Hue-preserving color image enhancement without gamut problem, IEEE Trans. Image Process. 12 (December (12)) (2003) 1591–1598.

[13] Q. Chen, X. Xu, Q. Sun, D. Xia, A solution to the deficiencies of image enhancement, Signal Process. 90 (2009) 44–56.

[14] C.-M. Tsai, Z.-M. Yeh, Y.-F. Wang, Decision tree-based contrast enhancement for various color images, Mach. Vis. Appl. 22 (1) (2009) 21–37.

[15] A. Ardeshir Goshtasby, Fusion of multi-exposure images, Image Vis. Comput. 23 (2005) 611–618.

[16] K.-Q. Huang, Q. Wang, Z.-Y. Wu, Natural color image enhancement and evaluation algorithm based on human visual system, Comput. Vis. Image Underst. 103 (2006) 52–63.

[17] L.A. Zadeh, Outline of a new approach to the analysis of complex systems and decision processes, IEEE Trans. Syst. Man Cybern. SMC-3 (January (1)) (1973) 28–44.

[18] M. Russo, G. Ramponi, A fuzzy operator for the enhancement of blurred and noisy images, IEEE Trans. Image Process. 4 (August (8)) (1995) 1169–1174.

[19] Y.S. Choi, R. Krishnapuram, A robust approach to image enhancement based on fuzzy logic, IEEE Trans. Image Process. 6 (June (6)) (1997) 808–825.

[20] C. Limei, Q. Jiansheng, Night color image enhancement using fuzzy set, in: International Conference on Image and Signal Processing, 2009, pp. 1–4.

[21] F. Kang, Y. Wang, Y. Zhao, The enhancement of fire color image based on an improved fuzzy algorithm, in: Internal Conference on Information Engineering and Computer Science, 2009, pp. 1–4.

[22] D.-L. Peng, A.-K. Xue, Degraded image enhancement with applications in robot vision, in: IEEE International Conference on Systems, Man and Cybernetics, 2, 2005, pp. 1837–1842.

[23] M. Hanmandlu, D. Jha, R. Sharma, Color image enhancement by fuzzy intensification, Pattern Recognit. Lett. 24 (2003) 81–87.

[24] M. Hanmandlu, S.N. Tandon, A.H. Mir, A new fuzzy logic based image enhancement, Biomed. Sci. Instrum. 34 (1997) 590–595.

[25] Sarode M.K.V., S.A. Ladhake, P.R. Deshmukh, Fuzzy system for color image enhancement, Eng. Technol. World Acad. Sci. (2008).

[26] H.D. Cheng, Y.-H. Chen, Y. Sun, A novel fuzzy entropy approach to image enhancement and thresholding, Signal Process. 75 (1999) 277–301.

[27] D. Yu, L.-H. Ma, H.-Q. Lu, Normalized SI correction for hue-preserving color image enhancement, in: 6th International Conference on Machine Learning and Cybernetics, 2007, pp. 1498–1503.

[28] R. Annamaria, Varkonyi-Koczy, Improved fuzzy logic supports HDR colored information enhancement, in: International Conference on Instrumentation and Measurement Technology, 2009, pp. 361–366.

[29] G. Deepak, L. Joonwhoam, Color image enhancement in HSV space using nonlinear transfer function and neighborhood dependent approach with preserving details, in: 4th Pacific-Rim Symposium on Image and Video Technology, 2010, pp. 422–426.

[30] M.-S. Shyu, J.-J. Leou, A genetic algorithm approach to color image enhancement, Pattern Recognit. 31 (7) (1998) 871–880.

[31] M. Dorigo, L.M. Gambardella, Ant colony system: a cooperative learning approach to the traveling salesman problem, IEEE Trans. Evol. Comput. 1 (1997) 53–66.

[32] M. Dorigo, V. Maniezzo, A. Coloni, Ant system: optimization by a colony of cooperation agents, IEEE Trans. Syst. Man Cybern. B 26 (1996) 29–41.

[33] T. Stutzle, H. Holger, Max–Min ant system, Future Gener. Comput. Syst. June (16) (2000) 889–914.

[34] H. Li, S. Ziong, On ant colony algorithm for solving continuous optimization problem, in: IEEE International Conference on Intelligent Information Hiding and Multimedia Signal Processing, 2008, pp. 1450–1453.

[35] J. Yang, Y. Zhuang, An improved ant colony optimization algorithm for solving a complex combinatorial optimization problem, Appl. Soft Comput. 10 (March (2)) (2010).

[36] V. Maniezzo, M. Milandri, An ant-based framework for very strongly constrained problems, in: Proceedings of ANTS2000, 2002, pp. 222–227.

[37] Y.C. Liang, A.E. Smith, An ant colony optimization algorithm for the redundancy allocation problem (RAP), IEEE Trans. Reliab. 53 (3) (2004) 417–423.

[38] R.S. Parpinelli, H.S. Lopes, A.A. Freitas, Data mining with an ant colony optimization algorithm, IEEE Trans. Evol. Comput. 6 (4) (2002) 321–332.

[39] Das. Lu, C.C. Chen, Edge detection improvement by ant colony optimization, Pattern Recognit. Lett. 29 (4) (2008) 416–425.

[40] H. Nezamabadi-Pour, S. Saryazdi, E. Rashedi, Edge detection using ant algorithm, Soft Computing 10 (2006, May) 623–628.

[41] A. Jevtić, D. Andina, Adaptive artificial ant colonies for edge detection in digital images, in: IECON, IEEE 2010, 2010, pp. 2813–2816.

[42] J. Zhang, K. He, J. Zhou, M. Gong, Ant colony optimization and statistical estimation approach to image edge detection, in: WiCOM IEEE 2010, 2010, pp. 1–4.

[43] J. Tian, W. Yu, S. Xie, An ant colony optimization algorithm for image edge detection, in: IEEE Congress on Evolutionary Computation, 2008, pp. 751–756.

[44] O.P. Verma, M. Hanmandlu, A.K. Sultania, Dhruv, A novel fuzzy ant system for edge detection, Computer and Information Science (ICIS), in: 2010 IEEE/ACIS 9th International Conference, 2010, pp. 228–233.

[45] O.P. Verma, M. Hanmandlu, P. Kumar, S. Shrivastava, A novel approach for edge detection using ant colony optimization and fuzzy derivative technique, in: IEEE International Advance Computing Conference, 2009, 2009, pp. 1206–1212.

[46] S. Meshoul, M. Batouche, Ant colony system with extremal dynamics for point matching and pose estimation, in: Proceeding of the 16th International Conference on Pattern Recognition, 3, 2002, pp. 823–826.

[47] M. Hanmandlu, D. Jha, An optimal fuzzy system for color image enhancement, IEEE Trans. Image Process. 15 (10) (2006) 2956–2966.

[48] M. Dorigo, G.D. Caro, Ant colony optimization: a new meta-heuristic, in: Proceedings of the Congress on Evolutionary Computation, IEEE, 1999, pp. 1470–1477.

[49] M. Dorigo, V. Maniezzo, A. Colorni, The Ant Sys-tem: optimization by a colony of cooperating agents, IEEE Trans. Syst. Man Cybern. B 26 (1) (1996) 29–41.